Molecular dynamics simulation of crystal growth in $Al_{50}Ni_{50}$: The generation of defects

Philipp Kuhn[1] and Jürgen Horbach[2]

[1]*Institut für Materialphysik im Weltraum, Deutsches Zentrum für Luft- und Raumfahrt (DLR), 51170 Köln, Germany*

[2]*Institut für Theoretische Physik II: Weiche Materie, Heinrich Heine-Universität Düsseldorf,*

Universitätsstraße 1, 40225 Düsseldorf, Germany

The ordering processes in the interface of a solidifying binary alloy ($Al_{50}Ni_{50}$) are studied by molecular dynamics computer simulation. At various temperatures below the melting point, inhomogeneous systems with planar crystal-melt interfaces in (100) orientation are prepared. The growth of a new crystalline Al or Ni layer proceeds through different time-delayed ordering processes. Before the onset of crystallization, there is a segregation process of Al and Ni atoms in the region where a new layer forms. We show that the interplay between segregation and crystallization supports the formation of a high nonequilibrium concentration of point defects.

PACS number(s): 68.08.De, 05.10.−a, 81.10.Fq

I. INTRODUCTION

The growth of a crystal in an undercooled melt is governed by processes within the interface between the solid and the liquid.[1,2] To obtain a microscopic understanding of these processes, an analysis of the structural changes that occur in the interfacial region during growth is required. For metallic alloys, however, information about the interfacial properties is hardly accessible from experiments and insight into these matters owes a lot to computer simulation studies.[3] So far, such investigations were mostly concerned with more global characteristics like the growth velocity[4–9] or static structural properties like the shape of the density profile in the interfacial region.[10–12]

In this study, we use molecular dynamics (MD) simulation of a realistic model of the binary system Al-Ni to investigate—on a particle level—the structural changes in a rough solid-liquid interface during growth. The underlying interaction model developed by Mishin *et al.*[13] was carefully designed to accurately reproduce the energetic and structural properties of the solid phase and as shown in Ref. 14, it additionally shows good agreement with experimentally obtained transport properties of the liquid phase. The interface of the B2 intermetallic crystal phase $Al_{50}Ni_{50}$ with the melt of the same composition is considered. To keep the setting simple, we consider a planar interface with a homogeneous temperature distribution, an idealization that can be thought of as a local section of a more realistic interface.

We find a remarkable interplay between chemical and geometrical[15] ordering processes within the interface that can leave imprints on the microstructure of the emerging solid. During the growth of a new crystalline Al or Ni layer, two aspects of the ordering process can be identified that set in at different times. First, Al and Ni atoms start to segregate in the region where the new layer forms, followed, in a second step, by the onset of crystallization. At the late stage of the crystallization of a layer, the concentration change is inhibited leading to the formation of a high nonequilibrium concentration of defects (of the order of a few percent) which increases with increasing undercooling. It is to be expected that some of these defects will heal out on a longer time

scale during a secondary relaxation stage. In that sense, we observe a distinct primary structure that is generated directly during growth. Since it is this immediate phase that determines the solidification pattern, this observation has important implications for the resulting microstructure. Furthermore, the defects strongly affect the material properties of the solid.[16–18]

Our results provide a basis for the modeling and further theoretical understanding of the growth of rough crystal-liquid interfaces in metallic alloys. Whether the interface is rough or faceted[1,19] is a decisive factor for the growth behavior and the resulting morphology. In the faceted case, the modeling of the principal growth mechanisms was established through the seminal work of Burton *et al.*[20] In their model, there are preferential binding sites at the surface of the crystal where single atoms attach, and so the growth of the crystal takes place via the transport to these sites and subsequent attachment/detachment events.

For rough interfaces, a single-particle picture is not adequate anymore. Due to thermal fluctuations along the interface there is an abundance of possible binding sites for the particles and growth is not limited by nucleation of new layers or the presence of inhomogeneities such as step edges. Rather than driven by attachment of single atoms, changes in the structure of rough interfaces are associated with cooperative rearrangements of particles.

The intermetallic compound $Al_{50}Ni_{50}$ is a suitable model system for studying rough interfaces. It constitutes an azeotrope where at the melting point the B2 crystal is at coexistence with a melt of the same composition. This has the advantage that no chemical partitioning introduces complications. In the B2 structure, each of the two atomic species occupies a simple cubic sublattice. For the (100) direction, this leads to a simple compositional pattern, consisting of alternating layers of Al and Ni. Regarding the lattice structure, these layers are equivalent and the chemical order is superimposed on the purely geometrical one. Therefore we analyze the interfacial structure layers with respect to composition and degree of crystallinity. This analysis allows for a detailed description of dynamic changes in the structure within the interface.

II. DETAILS OF THE SIMULATION

Newton's equations of motion are integrated using the velocity form of the Verlet algorithm with a time step $\delta t = 1$ fs. Periodic boundary conditions are imposed in all three spatial directions. To model the interactions between the ions in $Al_{50}Ni_{50}$, an embedded atom method (EAM) potential[13] is employed. To keep the temperature T constant, the system is coupled to a stochastic heat bath, generating every 200 time steps new velocities from a Maxwell-Boltzmann distribution.[21] Constant zero pressure ($p = 0$) is realized by a first-order barostat,[22] contracting or expanding the dimensions L_α ($\alpha = x, y, z$) of the simulation box uniformly in all three directions for equilibration or only in z direction (growth direction) for simulations of crystal growth. We refer to these runs as NpT and Np_zT runs, respectively (with N the total number of particles).

The starting configuration for all simulations is a perfect crystal with B2 structure and lattice constant 2.9 Å in a simulation box of size $L \times L \times 5L$. Similar to our recent work,[23,24] inhomogeneous systems at target temperature T and pressure $p = 0$ are prepared such that the system consists of ordered and disordered domains of approximate lengths $\frac{2}{5}L_z$ and $\frac{3}{5}L_z$, respectively. These domains are separated from each other by two planar interfaces.

The local degree of crystallinity is quantified by the bond order parameter q_6q_6,[23–25] a variant of the rotationally-invariant order parameters introduced by Steinhardt *et al.*[26] Based on the geometrical shape of its neighborhood, a value is assigned to each particle that allows a discrimination of liquid and solid local order. Neighboring particles within a distance of 3.6 Å are taken into account, corresponding to a radius that spans the first neighbor shells of both liquid and solid particles. For the B2 structure, one can either take into account all neighbors or only those of the same species, thus measuring the local order within the two sublattices. In the following, we will use the first alternative but our results do not depend on this choice.

For the crystal growth simulation, in z direction the system is coupled to a thermostat and a barostat. This is necessary since during growth latent heat is released and the sample as a whole contracts in z direction because the density of the solid is higher than that of the liquid. Since this shrinkage accurately reflects the increase of the solid/liquid ratio in the system, we can actually use the rate of contraction to infer the velocity v_I with which the interface moves. From this, the melting temperature can be determined as the temperature $T_m \simeq 1545$ K at which the velocity becomes zero. The inset of Fig. 1 shows the growth velocity as a function of undercooling $\Delta T = T_m - T$. As expected, for small undercooling, the dependance is linear, whereas at the highest considered value, $\Delta T = 95$ K, there is already a visible deviation from linear behavior.

The simulations were carried out with $N = 21\,970$ particles. We also did a test with a particle number of 106 480 in order to ensure that the reported effects are not artifacts due to the system size.

III. RESULTS

Within the interfacial region, the degree of structural and chemical order exhibits considerable variation. Accordingly,
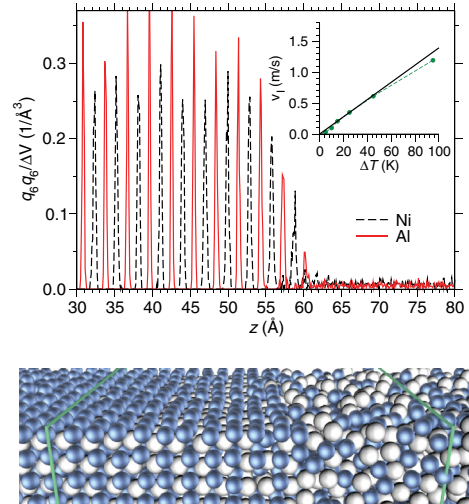
FIG. 1. (Color online) Order parameter profile of the interfacial region with a section of the corresponding atomic configuration at $T = 1500$ K (blue particles are Ni and white ones Al; the green lines mark the z range depicted in the profile plot). The inset shows the interface velocity v_I as a function of undercooling ΔT. The solid line is a linear fit to the data for small ΔT.

the local environment for the particles and their possibilities of rearrangement is highly nonuniform. For an analysis, some degree of coarse graining is required to extract useful observables but the difficulty lies in the right choice of this coarse graining that should preserve the essential information about the heterogeneity. Since the growing interface consists of layers, as it is clearly visible in Fig. 1, we use them as natural structural units and introduce observables by taking averages over single layers. This is similar to the analysis employed by Nada *et al.*[27] to study the growth of ice layers.

For the B2 structure, the quest for the particles to form a regular arrangement is complicated by the presence of two sublattices. For the (100) direction, this feature is evident on the level of the layers because each layer has to collect one of the two species and repel the other one such that the crystal can be formed. Thus the ordering process involves two interwoven aspects: a compositional segregation and the actual formation of the lattice structure. At each instant, we monitor the fraction of Al and Ni particles in a given layer, x_α ($\alpha = Al, Ni$), and the average degree of crystallinity in the layer by q_6q_6. For the latter, we sum over all particles in a layer, normalize to the value of a perfect crystal at that temperature and denote the resulting quantity by $(q_6q_6)^*$.

The results for x_α and $(q_6q_6)^*$ for the three undercoolings $\Delta T = 25$, 45 and 95 K are shown in Fig. 2. Each curve is an average over 50 layers. The time axis is rescaled by the growth velocity and the resulting collapse shows that the rates of both processes are set by the overall pace of the interface drift and increasing the undercooling merely causes a shrinking of this fundamental time scale. This rescaling is actually a natural one since for stationary growth spatial and temporal behavior are connected by a traveling wave relation $\Phi(z - v_I t)$ and the growth velocity translates between space and time domain.

The behavior of x_α and $(q_6q_6)^*$ can be understood through a intuitive picture of the interplay between segregation and
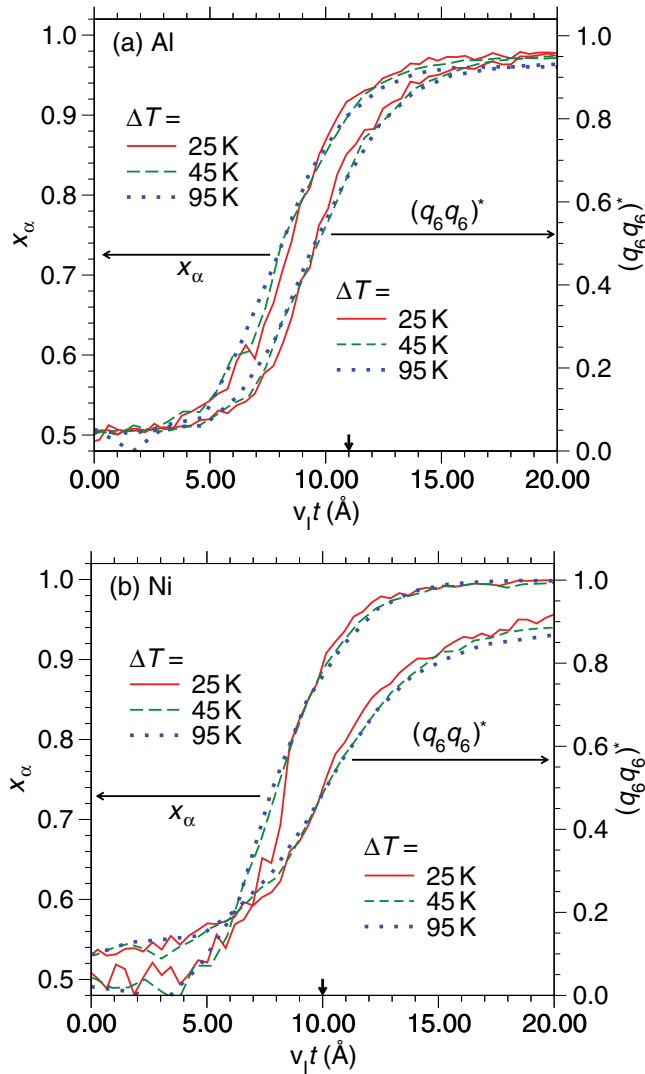
FIG. 2. (Color online) Concentration x_α ($\alpha = $ Ni, Al) and order parameter $(q_6 q_6)^*$ (see text) for (a) Al and (b) Ni as a function of rescaled time $v_l t$ for different undercoolings, as indicated. Note that x_{Al} and $(q_6 q_6)^*$ for Al and Ni do not reach the value of a perfect crystal because of structural defects. The bold arrows on the x axes mark the time $t = 320$ ps at $\Delta T = 95$ K (see corresponding snapshots in Fig. 3).

FIG. 3. (Color online) Snapshots of crystalline Ni (left) and Al layers (right) at $t = 192, 320$, and 700 ps (top down) resulting from the planar growth from the melt at $\Delta T = 95$ K. Blue and white spheres correspond to Ni and Al atoms, respectively. To provide a visual accentuation of crystalline configurations, particles with $q_6 q_6 < 0.6$ (liquid) are depicted semitransparent.

crystallization. Larger crystalline islands (cf. Fig. 3) only form after a certain accumulation of one species in a layer has taken place. After these islands stabilize, further crystallization proceeds rather rapidly. On the other hand, compositional ordering is more and more suppressed since the solidified domains pin the particles to their respective layers. This interference between compositional and crystalline ordering gives rise to an interesting phenomenon: the appearance of structural defects. In the almost completely crystallized layers, mass transport is effectively prohibited and the residual defects cannot heal out on the time scale of solidification.

Figure 3 shows the time evolution of a typical Ni and Al layer at $\Delta T = 95$ K. In the final state, the dominant defects are vacancies in the Ni layer (V_{Ni}) and Ni_{Al} antisites (Ni atoms on the Al sublattice). This is reminiscent of the triple-defect model[28–30] where two vacancies on the Ni sublattice are

compensated by an antisite on the Al lattice to preserve the 50/50 composition of the crystal. In our case, there is a small excess of V_{Ni} that increases with undercooling so the crystal actually grows at a composition that is slightly on the Ni-rich side. This leads to an accumulation of Al in the melt, so we had to restrict our analysis to only a few layers in each simulation run to ensure that this does not affect the growth.

It should be emphasized that although for entropic reasons the crystal is expected to contain a certain degree of disorder, the defects in Fig. 3 arise from a different origin. Figure 4 shows the concentration of the various defects as a function of undercooling. For small undercooling, the ratio of V_{Ni} and Ni_{Al} seems to approach a value close to two, consistent with the triple-defect mechanism. For higher undercooling, the concentrations of these two defects become nearly equal, leaving a net surplus of Ni, which is the deviation from stoichiometry mentioned above. Most obviously, the defect concentrations *increase* with decreasing temperature and
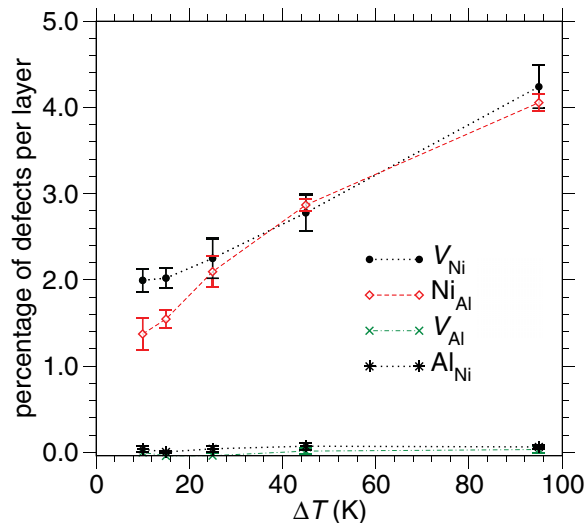
FIG. 4. (Color online) Percentage of defects per layer as a function of undercooling. For an explanation of the different types of defects, see text. The scattering of the values from different simulation runs is indicated by error bars.

therefore indicate its origin in the nonequilibrium growth kinetics. More specifically, the following interaction between fluctuation and drift takes place: the thermal interface fluctuations allow the system to probe configurations in an energy landscape with many local minima, including configurations with defects such as antisites. Particles are shuffled around and tend to stick in places that lower the free energy of the system and thermal fluctuations help to shake free particles that are trapped at unfavorable positions. If the system is brought to a finite undercooling, the fluctuations persist but the interface starts to propagate. The faster the interface moves the fewer times the atoms detach and reattach before they can be incorporated into the crystal and thus imperfections freeze in.

IV. CONCLUSIONS

In conclusion, we have presented a MD simulation of crystal growth in $Al_{50}Ni_{50}$ using an EAM potential to model the interactions between the particles. A layer analysis of the rough interface between the B2 phase of $Al_{50}Ni_{50}$ with the melt of the same composition has been carried out. We have shown that there is a two-step ordering process during the formation of a new crystalline layer where the segregation of the different species precedes the onset of crystallization. The latter ordering processes during interface growth determine the structure of the growing solid and may have consequences on the microstructure and the resulting mechanical properties. For $Al_{50}Ni_{50}$, we have revealed a high concentration of point defects. Similar features may also occur in other metallic systems since the basic interplay between segregation and crystallization during crystal growth just requires different species with a strong chemical ordering.

As a final remark, we comment on possible experimental tests of our results. The most distinctive observable feature in our simulations is the growth of a nonstochiometric phase, accompanied by the accumulation of Al in the melt. The deviations from the stoichiometric composition are in the percent range and should lead to an inhomogeneous concentration profile ahead of the solidification front. The new generation of *in situ* x-ray radiography[31,32] is capable of resolving such an effect and could provide at least a qualitative assessment of our predictions.

ACKNOWLEDGMENTS

[1]D. P. Woodruff, *The Solid-Liquid Interface* (Cambridge University Press, Cambridge, 1980).

[2]*Solidification of Containerless Undercooled Melts*, edited by D. M. Herlach and D. M. Matson (Wiley VCH, Weinheim, 2012).

[3]G. H. Gilmer, *Handbook of Crystal Growth*, edited by D. T. J. Hurle (Elsevier, Amsterdam, 1993), Vol. 1.

[4]J. Q. Broughton, G. H. Gilmer, and K. A. Jackson, Phys. Rev. Lett. **49**, 1496 (1982).

[5]E. Burke, J. Q. Broughton, and G. H. Gilmer, J. Chem. Phys. **89**, 1030 (1988).

[6]W. J. Briels and H. L. Tepper, Phys. Rev. Lett. **79**, 5074 (1997).

[7]M. Amini and B. B. Laird, Phys. Rev. Lett. **97**, 216102 (2006).

[8]J. J. Hoyt and M. Asta, Phys. Rev. B **65**, 214106 (2002).

[9]D. Y. Sun, M. Asta, and J. J. Hoyt, Phys. Rev. B **69**, 024108 (2004).

[10]J. Q. Broughton and G. H. Gilmer, J. Chem. Phys. **84**, 5749 (1986).

[11]H. E. A. Huitema, M. J. Vlot, and J. P. van der Eerden, J. Chem. Phys. **111**, 4714 (1999).

[12]R. L. Davidchack and B. B. Laird, J. Chem. Phys. **108**, 9452 (1998).

[13]Y. Mishin, M. J. Mehl, and D. A. Papaconstantopoulos, Phys. Rev. B **65**, 224114 (2002).

[14]J. Horbach, S. K. Das, A. Griesche, M.-P. Macht, G. Frohberg, and A. Meyer, Phys. Rev. B **75**, 174304 (2007).

[15]By geometrical order we mean the purely structural aspect that does not discern between different species.

[16]I. Baker, Mater. Sci. Eng. A **192–193**, 1 (1995).

[17]L. M. Pike, I. M. Anderson, C. T. Liu, and Y. A. Chang, Acta Mater. **50**, 3859 (2002).

[18]D. B. Miracle, Acta Metal. Mater. **41**, 649 (1993).

[19]K. A. Jackson, Prog. Solid State Chem. **4**, 53 (1967).

[20]W. K. Burton, N. Cabrera, and F. C. Frank, Philos. Trans. R. Soc. London A **243**, 299 (1951).

[21]D. Frenkel and B. Smit, *Understanding Molecular Simulation: From Algorithms to Applications*, 2nd ed. (Academic Press, San Diego, 2001).

[22]H. J. C. Berendsen, J. P. M. Postma, W. F. van Gunsteren, A. Dinola, and J. R. Haak, J. Chem. Phys. **81**, 3684 (1984).

[23]R. E. Rozas and J. Horbach, Europhys. Lett. **93**, 26006 (2011).

[24]A. Härtel, M. Oettel, R. E. Rozas, S. U. Egelhaaf, J. Horbach, and H. Löwen, Phys. Rev. Lett. **108**, 226101 (2012).

[25] P. R. ten Wolde, M. J. Ruiz-Montero, and D. Frenkel, Phys. Rev. Lett. **75**, 2714 (1995).

[26] P. J. Steinhardt, D. R. Nelson, and M. Ronchetti, Phys. Rev. B **28**, 784 (1983).

[27] H. Nada, J. P. van der Eerden, and Y. Furukawa, J. Cryst. Growth **266**, 297 (2004).

[28] A. J. Bradley and A. Taylor, Proc. R. Soc. A **159**, 56 (1937).

[29] R. J. Wasilewski, J. Phys. Chem. Solids **29**, 39 (1968).

[30] P. A. Korzhavyi, A. V. Ruban, A. Y. Lozovoi, Y. K. Vekilov, I. A. Abrikosov, and B. Johansson, Phys. Rev. B **61**, 6003 (2000).

[31] B. Zhang, A. Griesche, and A. Meyer, Phys. Rev. Lett. **104**, 035902 (2010).

[32] B. Billia, H. Nguyen-Thi, N. Mangelinck-Noel, N. Bergeon, H. Jung, G. Reinhart, A. Bogno, A. Buffet, J. Hartwig, J. Baruchel, and T. Schenk, ISIJ Int. **50**, 1929 (2010).